JMES

# Removal of humic acids on iron pillared clay suspensions by ultrafiltration/photocatalysis hybrid method

## W. Benlemmane, M. W. Naceur, S. Soukane

*Department of Process Engineering, University of Saâd Dahlab Blida 1, PO .box 270, 09000 Blida, Algeria.*
*Laboratoire des Applications énergétiques de l'hydrogène LApEH*

## Abstract

Iron pillaring of mineral clay particles was carried out for catalyst preparation used in the removal of humic substances from aqueous solution. The catalysts were characterized by XRD, BET, and IR methods. The present study explores firstly the efficiency of photocatalytic oxidation of humic acids (HA), which are typical refractory components of Natural Organic Matter (NOM). The effects of solution pH, HA concentration, and catalyst loading on the photodegradation of HA were examined. Ultrafiltration (UF) has become one of the best alternatives replacing conventional drinking water treatment technologies because of severe regulations for drinking water quality. However, membrane fouling is an important factor which limits its widespread application. The successful operation of a hybrid photocatalysis–membrane separation process is proved at the laboratory scale for degradation of Humic Acids (HA). The global process removal efficiency (comprising both HA oxidation and UF membrane rejection) is higher than conventional UF, as a result of the synergistic effects of both photocatalytic oxidation and membrane filtration.

## 1. Introduction

Humic substances are complex heterogeneous acidic biopolymers that represent a significant fraction of Natural Organic Matter (NOM) present in freshwater sources [1-4]. They are produced in water by microbiological reactions responsible for the decay of tissues of dead plants and animals [5]. Humic substances are a primary target in water treatment processes even though they are not considered pollutants [6]. Negative effects of humic substances in drinkable water include undesirable color and taste, absorption and concentration of organic pollutants, as well as biochemical decomposition in water distribution systems. Moreover, NOM can act as a precursor for the formation of Disinfection By-Products (DBPs) during common chlorination of drinking water [7]. Severe health effects associated with DBPs led several countries to take specific measures to ensure control of DBPs and their precursors (NOM) [2].

Besides conventional treatment processes (e.g. coagulation/flocculation[8, 9], ion exchange[10] and activated carbon adsorption [2]), advanced oxidation techniques are considered as effective tools for the elimination of humic acids (HAs) from natural waters [3]. Those processes can be divided into homogeneous ones – chemical oxidation (ozone, hydrogen dioxide) and heterogeneous ones – UV radiations at the presence of catalysts [5]. The photocatalysis technology can destroy the organic contaminants totally to $CO_2$ and $H_2O$, and it has other several advantages, such as no waste disposal problem, no expensive oxidants needed, low costs, and only mild temperature and pressure [11]. Heterogeneous photocatalytic oxidation is considered one of promising and green techniques for water treatment as well as it has been the subject of a wide range of researches [12]. However, up to now no interest was shown for the use of inorganic colloidal matter i.e. pillared clay mineral particles as photocatalysts in the photodegradation of humic acids.

Bentonite is one of the most widely used low-cost clays due to its abundant availability. It's composed mainly of montmorillonite [13, 14] and considered one of the most common industrial.Its unit layer structure consists of two sheets of silicon atoms tetrahedrally coordinated with oxygen sandwiching a sheet of aluminum atoms octahedrally coordinated with oxygen. Divalent $Fe^{2+}$ or $Mg^{2+}$ ions sometimes replace the $Al^{3+}$ in the octahedral sheet, and $Al^{3+}$ can be substituted for $Si^{4+}$ in the tetrahedral layer. These cations are exchangeable with certain other kinds of inorganic and/or organic polycations, resulting in pillared materials [15].

The pillared clays have a vast range of potential applications in catalytic process [16]. Pillared clays (PILCs) are formed by exploiting the expandability and cation exchange of smectites. Large hydroxyl polycations can be intercalated through cation exchange into the interlayer space of the clay followed by calcinations, to transform hydroxyl polycations into stable pillars [17]. PILCs have a microporous structure; high specific surface areas and high thermal stabilities. Both Brønsted and Lewis acid sites are present. A variety of pore dimensions and catalytic activities are available depending on the type of PILCs [18]. The physico-chemical properties of PILCs may vary depending on the pillar species used. Thus, pillared derivatives of clays have received widespread interest as a new type of layered material that can serve as shape-selective catalysts, separating agents, supports, and sorbents [19]. The metal hydroxy cations undergo dehydration and dehydroxylation and are transformed to metal oxide (e.g., $Al_2O_3$ and $Fe_2O_3$) clusters/nanoparticles, which act as pillars to prop the clay mineral layers apart, and to produce a stable microporous pillared structure. The resultant oxide-PILC has shown some promising prospects in the fields both of adsorbents and catalysts. A common way to synthesize $Fe_2O_3$-PILC is based on the intercalation of iron polycations, the base-hydrolyzed product of Fe(III) salts, such as $FeCl_3$ and $Fe(NO_3)_3$[20].

The iron in PILC is stable against changes in solution pH and shows only limited leaching. Moreover, the strong surface acidity of some Fe-PILC permits catalytic activity to be maintained over a large range of pH values [21]. Low-pressure membrane filtration has been considered as a promising technology for water treatment in the 21st century. With the decreasing cost of the ultrafiltration membrane, UF technology is progressively accepted by the developing countries compared to other low-pressure membrane technologies, and is expected to be more widely applied due to the more severe water environment [22]. The membrane fouling is still the most limiting factor for wider application of ultrafiltration. Accumulation of foulants on the membranes' surfacehighly influences the lifetime of membrane and decreases the permeate flux, which increases the required pressure and energy for the membrane to operate [23].

An interesting solution in water treatment technology is to use a so called hybrid system that combines photocatalysis with membrane filtration (microfiltration, ultrafiltration or nanofiltration) [5]. In such systems, the contaminants could be decomposed into simple compounds by photooxidation, while the photocatalyst could be separated by the used membrane.

The objective of this study is to investigate the influence of modified Algerian montmorillonite on the hybrid photocatalysis-membrane filtration process and its use for the removal of HA. Bentonite abundance in Algeria is estimated at millions tons and is currently introduced in different industries [24]. The effects of photocatalyst concentration, substrate concentration, medium pH and irradiation times on the HA removal have been examined. In this study, an integrated photocatalysis-membrane hybrid system was used to remove HA in water. This system was chosen because it is relatively cheap, easy to set up and also able to reduce the fouling of the membrane. Photocatalytic reaction degrades the foulant in wastewater, and hence reduces the foulant on the membrane surface.

## 2. Material and Methods
### 2.1. Synthesis and characterization of the photocatalyst
The iron-modified pillared montmorillonite powder was synthesized according to previous reported methods [25-27]. The crude bentonite (Maghnia deposit from the west of Algeria), supplied by ENOF (Entreprise Nationale des Substances Utiles et des Produits Non Ferreux, Algeria), was used as the starting material to prepare a modified pillared montmorillonites. Clay particles with size less than 2 μm were converted into homoionic form by adding appropriate amounts of 1 mol $L^{-1}$ NaCl solution to replace all exchangeable cations with $Na^+$. After five successive NaCl treatments, the homoionic clay was freed from anions by several dialysis cycles in deionised water. The iron pillaring solution which gives Fe-hydroxy polymer was aged at room temperature for 10 days [25]. The intercalation of montmorillonite (Mt) by the pillaring solutions was obtained using the following parameters: the final concentration $[Fe]_f$ = 0.2 M, molar ratio OH/Fe = 2, Fe/Mt-Na ratio = 5 mmol.$g^{-1}$. Mt-Na suspension (1% (w/w)) was intercalated by iron polycations by adding drops of iron pillaring solution to homoionic montmorillonite suspension. After several filtration and washing cycles with distilled water, solid Mt-Fe was dried at 40°C for at least 72 h [27], then calcinated at 400 °C for 3 h and was finally ground and kept away from light. The crystalline structure was determined by X-ray diffraction (XRD) recorded on a PANalytical: XPERT-PRO powder diffractometer (Cu Kα radiation, λ = 1.5418 Å). Nitrogen physisorption was measured using a Micromeritics Nova 2000e, and Specific Surface Areas (SSA) values were calculated from the BET isotherm plots. FT-IR spectroscopy (using a Shimadzu type 8900 FT-IR spectrometer) was performed to identify the chemical functional groups present in the samples. The substance was finely ground and dispersed into KBr powder-pressed pellets. IR Transmittance data were obtained for wave numbers ranging from 4000 $cm^{-1}$ to 400 $cm^{-1}$.

## 2.2. Preparation of humic acids solution

The synthetic humic acids used are commercial products supplied by ACros. Base solution was prepared by dissolving 1g of humic acids into 62.5 ml of NaOH (2N) and then adding distilled water up to 1L. This solution was stirred for 24 h and stored at 4 °C away from light. Solutions of 10 mg/L were prepared by dilution from the base solution.

## 2.3. Photocatalytic techniques

A laboratory scale photoreactor (cylindrical batch reactor) with a volume of 2500 mL useful capacity (see Figure 1) was used for the photocatalytic investigation. The photocatalytic reactor was filled with 2000 mL of aqueous solution containing 10 mg/L of HA. UV irradiation was provided by a Philips immersion UV-A 24 W medium-pressure mercury lamp emitting UV radiation of wavelength 254 nm. The lamp was placed inside the reactor and was cooled with water to keep its temperature constant. Air was bubbled through the solution to ensure steady oxygen supply. The reactor content was stirred by means of a magnetic stirrer. The reactor external sidewalls were covered with aluminum foil. Diluted HCl or NaOH were used for initial pH adjustments. Thirty minutes away from light were allowed for adsorption to reach equilibrium, so that adsorption of HA on Fe-PILC can occur before irradiation. At this stage, the gas was bubbled through and the lamp allowed to warm up.
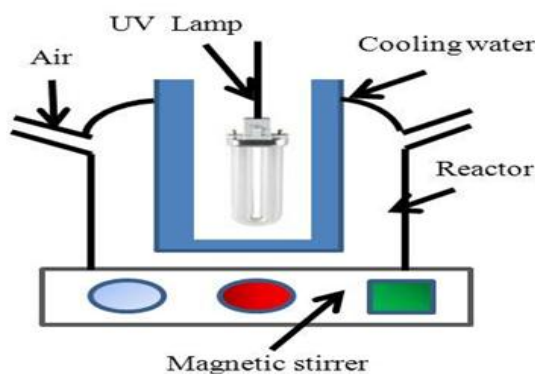


**Figure 1:** Description of the photocatalysis experimental set up.

Thereafter, 10 mL samples were collected at 30 min intervals and centrifuged twice during 30 minutes at 4000 rpm. Regarding the degradation of HA, $UV_{254}$ was measured in a 10 mm quartz cell in the Shimadzu UV-1800 spectrophotometer, as the concentration of HA in the solution changes with degradation. The impact of the following parameters on the photodegradation of humic acids in water solutions was investigated:
  - the presence of catalyst (photocatalysis, photolysis),
  - water pH (pH = 3.0; 5.0 and 10.9 (normal pH) )
  - catalyst amount (0.02; 0,03; 0.05 and 0.5 g/L),
  - Concentration of humic acids in water (5; 10; 15 and 20 mg/L).

The performance of ultrafiltration membrane was investigated by analyzing NOM removal and flux decline in dead-end filtration experiments.

## 2.4. Preparation of flat–sheet membranes

In this study an Amicon-Millipore 8200 filtration cell with a capacity of 200 mL was operated in dead-end mode, without stirring. A flat sheet polyethersulphone ultrafiltration membrane (molecular weight of 5 kDa) has been used in the filtration experimental. The system used for filtration is depicted in Figure 2. The filtration cell was connected to a $N_2$ gas source to induce pressure. Permeate was collected and the flux was measured. The effective surface areas of all the membranes were 28.7cm$^2$. All experiments were carried out at room temperature (25 ± 1°C). Membranes were used for filtration of humic acid solutions (10 mg/L, pH = 3.0). Water flux was measured periodically, and filtrate samples collected for subsequent analysis.

# 3. Results and discussion

## 3.1. Characterization of Fe-PILCs

Powder XRD patterns of the fresh catalyst (Figure 3) were similar to those reported in the literature for Fe-PILC [28]. The peak observed at 2θ = 7.17° of (Na- bentonite) was attributed to the basal space (001) reflection, which corresponds to a d-value of 1.233 nm. Pillaring with Fe the (001) produced a shift in reflections to lower 2θ values, corresponding to the increase in $d_{001}$ value; while the rest of the structures was not clearly affected.

However, a new reflection appeared at approximately 2θ = 5.76°, which corresponds to a d-value of 1.533 nm. The $d_{001}$ value of prepared pillared clay increased after pillaring from 12.33 to 15.33 Å, indicating intercalation by small polyhydroxymeric species of about 3 Å. The FT-IR spectra of these samples are depicted in Figure 4. After intercalation of the montmorillonite by the pillaring solution, the presence of iron in the pillared clay was confirmed by characteristic bands in the FTIR spectra.



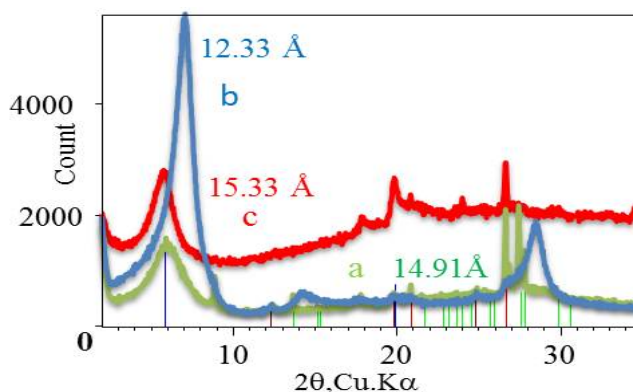**Figure 2**: Schematic diagram of flat-sheet UF system.



**Figure 3**: XRD patterns of the used samples: (a) original bentonite, (b) Mt-Na, (c) Mt-Feused samples.

Specific surface areas (SSA) were determined according to the Brunauer–Emmett–Teller (BET) protocol. The surface area was calculated from the adsorption data and results give 54 m$^2$/g for bentonite and 97 m$^2$/g for Mt-Fe.
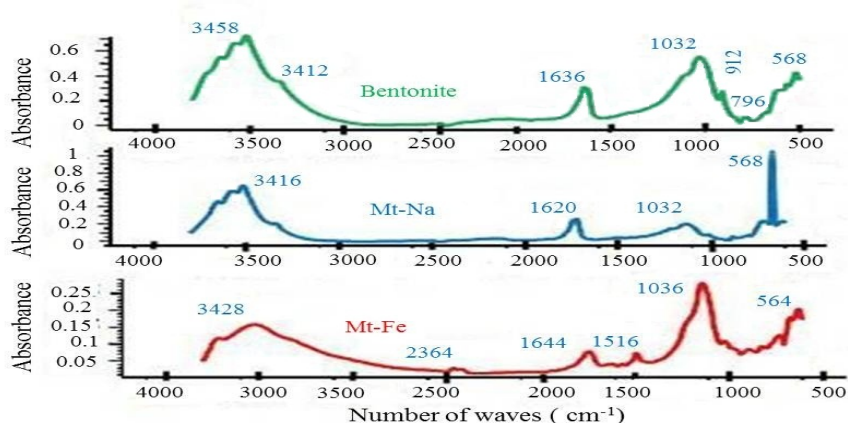


**Figure 4:** FT-IR spectra of the used samples.

### 3.2. Synergy between adsorption and photocatalytic degradation

The adsorption of humic acids onto Mt-Fe depends on the surface charge, hydrophobicity, substrate pores' structure and solution conditions. The contribution from adsorption, photo-degradation and photocatalytic degradation is important as shown in Figure 5. The adsorption experiments carried out in the dark using concentration C $_{(Mt\text{-}Fe)} \approx 0.05$ g.L$^{-1}$ at pH 3.0 showed that the adsorption equilibrium was reached within 30 min with an elimination of 28% of HA. The decrease of concentration of humic acids indicated that the adsorption of

organic contaminants on the catalyst surface was a crucial condition for an effective action of the photocatalyst. For all subsequent experiments, an adsorption time of 30 min was chosen to ensure saturation. The photolysis process based only on the decomposition at UV exposure was insufficient for the degradation of the investigated compound, while a more important decrease of the organic contaminant (HA) concentration was observed in the photocatalysis process.
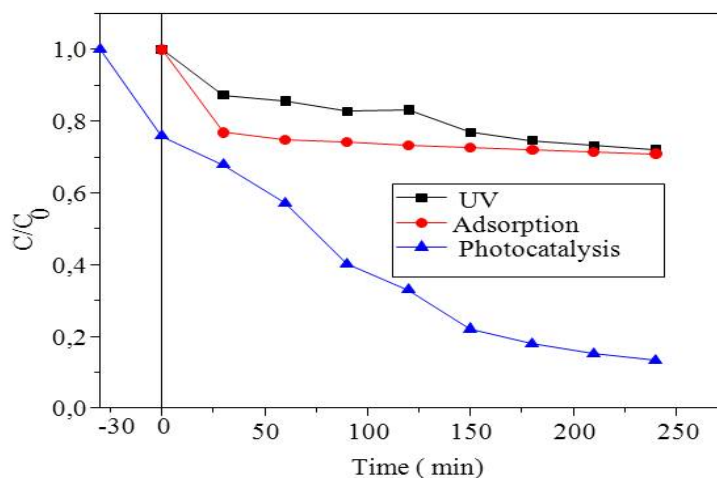


**Figure 5:** Reduction of HA under different experimental conditions: $[HA]_0$ = 10 mg/L; [Mt-Fe] = 0.05 g/L; pH = 3.0.

### 3.3. Influence of pH

In the photocatalytic system, the pH value is an important parameter for the determination of the properties of both the solid catalyst and the solute molecules. Indeed, pH can influence both photocatalytic reactions as well as the rate of adsorption on the photocatalyst surface. In this experiment, the initial concentration of HA was 10 mg/L and the Mt-Fe loading was 0.05 g/L. Results of the experiments at pH 3.0, 5.0 and 10.9, respectively, are represented in Figure 6.
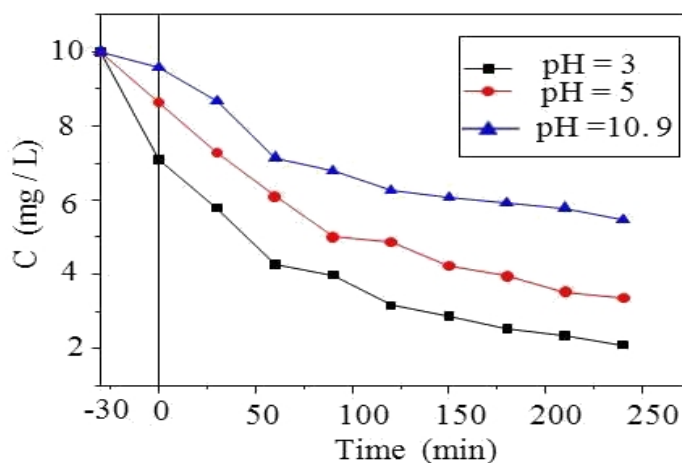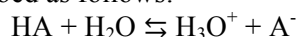


**Figure 6:** The effect of pH on the photodegradation of HA. ($[HA]_0$ =10 mg/L [Mt-Fe] = 0.05g/L).

The results indicate that pH has a significant effect, particularly at low values where the observed photodegradation rates were high. It is well established that macromolecules of humic acids contain conjugated olefinic, aromatic and phenolic–semiquinone–quinone structures of (–CO, –COOH, –OH, –NH–, –NH2, –N–) [29] , whereas during the pillaring process, the expansion in the clay structure contributed  to the enhancement of the specific surface area and porosity of the clay materials [19]. The point of zero charge (PZC) is a pH value at which the total amount of positive charge on the surface of solid is equal to the total amount of negative charge on it [30, 31]. It is well known that humic substances are weakly dissociable acids; the ionization is heavily dependent on pH and can be described as follows:

$$HA + H_2O \leftrightarrows H_3O^+ + A^-$$

The $pH_{pzc}$ of the Mt-Fe used in the study was around 6.9 [32].Increasing pH increases the ionization of humic substance and hence the concentration of negatively charged anion $A^-$. Above the $pH_{pzc}$ of 6.9 the clay surface is negatively charged. The increasing electrostatic repulsion between $A^-$ and clay particle would lead to reduced adsorption of humic substances, which affects negatively the photo-oxidation rates. If the pH <$pH_{pzc}$, the solutions produced more protons than the hydroxyl groups and the adsorbent surface would be positively

charged (cationic) and tend to attract anions [33], thus increasing the efficiency of HA degradation. The $pK_a$ values of acidic sites on various humic substances are generally in the range of 3-4.5. So, if solutions have pH larger than these $pK_a$ values, phenolic and carboxylic groups in the HA structure are ionized and HA becomes dominantly negatively charged [34]. Consequently, electrostatic attraction between surfaces positive charge Mt-Fe and surface negative charge of HA increases, hence removal of HA increases. These results show the surface charges of both HA and Mt-Fe changes, as a function of pH, and plays a vital role in the photocatalytic degradation.

### 3.4. Effects of photocatalyst concentration

Photocatalyst concentration is a major parameter which affects the photocatalytic oxidation rate. In order to avoid an excessive use of catalyst, it is necessary to find the optimum load for and efficient removal of HA [35]. To determine the influence of the catalyst concentration on the oxidation of humic acids, a series of experiments were carried out with various catalyst doses added to a solution with pH = 3.0. The results showed that degradation obtained for humic acids increases with a catalyst dose equal to 0.02 g Mt-Fe/L (Figure 7).
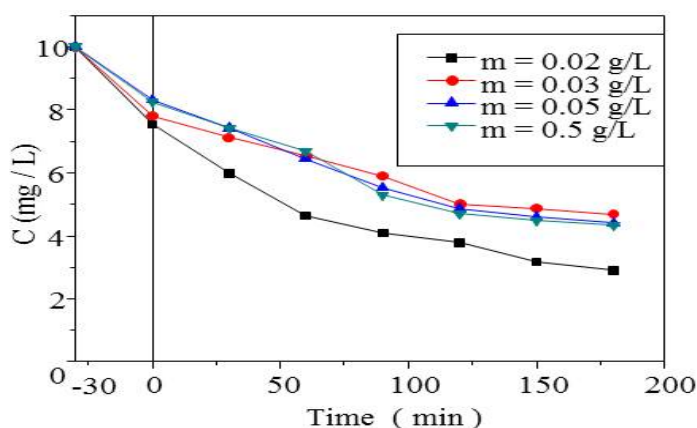


**Figure 7:** The effect of Mt-Fe concentration on the photodegradation of HA. ($[HA]_0$ =10 mgl/L, initial pH = 3.0).

When the catalyst concentration is greater than 0.02 g/L, degradation of HA decreases slightly. The observed decrease of reaction rate was probably due to the following reasons: as the catalyst concentration increases, the number of photons absorbed and the number of HA molecules adsorbed increase due to an increase in the number of catalyst particles. At a given level, the number of available substrate molecules is unable to sustain adsorption of an increasing number of Mt-Fe particles. Simultaneously, due to an increase in the turbidity of the suspension, there is a decrease in UV light penetration which enhances the scattering effect and decreases the photoactivated volume of the suspension. Therefore, above some level, additional particles are not involved in catalyst activity.

### 3.5. Effect of Substrate Concentration

### 3.5.1. Parametric study

Successful application of the photocatalytic oxidation requires the investigation of the dependence of photocatalytic degradation rate on substrate concentration. After optimizing the pH conditions and catalyst dose (pH 3.0 and catalyst dose 0.02 g/L) the photocatalytic degradation of HA was carried out by varying the initial concentrations of HA from 5 to 20 mg/L. Experimental results represented in Figure 8 show that the degradation rate depends on the initial concentration of humic acids. The main effect of increasing concentration is to increase the amount of substrate that is adsorbed onto the photocatalyst surface. If it is assumed that photocatalysis occurs at the surface, then the concentration of the substrate adsorbed to the surface has a direct effect on the overall rate of adsorption [36] and degradation.

Further increase of HA concentration decreases the rate of degradation. The color of the solution intensifies and the path length of photons entering the solution is shortened. Consequently, fewer photons reach the catalyst surface. Hence, the production of hydroxyl and superoxide radicals is reduced and the photodegradation efficiency is reduced as well. Moreover, at higher concentration, the number of collisions between HA molecules increases whereas the number of collisions between HA molecules and OH˙radicals decreases. Consequently, the rate of reaction is lowered. The rate of photocatalytic degradation of some pollutant depends on their nature, concentration and other existing compounds in the aqueous solution. At low concentrations, the

number of catalytic sites will not be a limiting factor, and the rate of degradation is proportional to the substrate concentration with apparent first-order kinetics.

The Langmuir-Hinshelwood (L-H) kinetics model is used to describe the dependence of the observed reaction rate on the initial solute concentrations, although the model parameters will be strongly dependent on the composition of the solution and other reactor operating conditions.
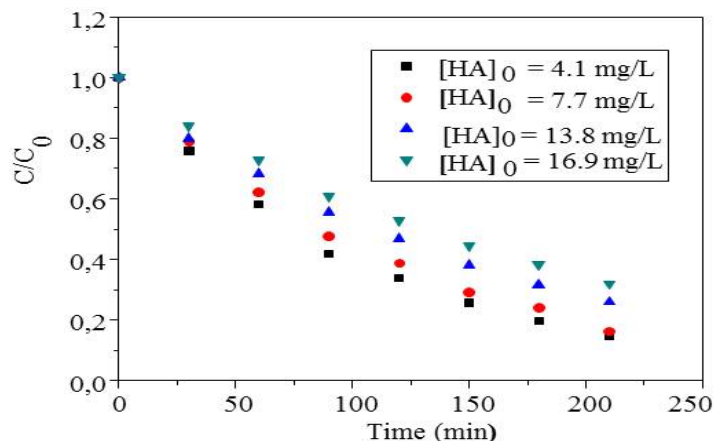


**Figure 8:** Evolution of the reduced concentration of humic acid versus time for different initial concentrations: Conditions [Mt-Fe] = 0.02 g /L and pH = 3.0.

### 3.5.2. Kinetic study

This set of photooxidation tests was performed to determine the kinetic constant of the first order reaction for the HA photodegradation with different initial HA concentration. Four tests with the same initial pH 3.0, Mt-Fe concentration of 0.02 $g.L^{-1}$, and different initial HA concentrations were conducted in the presence of UV irradiation. The tests duration was 3.5 h and samples for analysis were collected at different time intervals during the reaction. The experimental results are reported in Figure 9.
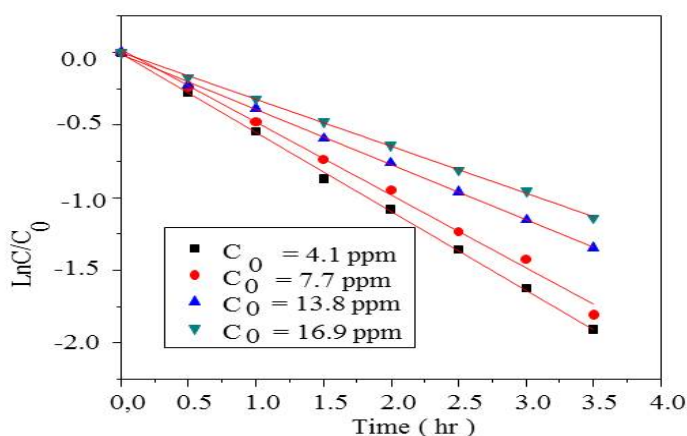


**Figure 9:** The Kinetic of photocatalytic degradation of the humic acid. First linear transform.
Ln $(C/C_0)$ = f (t). Conditions: pH 3.0, [Mt-Fe] = 0.02 g/L.

The Langmuir–Hinshelwood (LH) kinetic model has found widespread applications in investigations of advanced oxidation such as photocatalytic oxidation of organic substances [37]. When the initial concentration of HA was low, the L–H rate form reduced to an apparent first-order kinetics. If it is assumed that the photocatalytic degradation reaction of HA follows the first-order kinetics for $C_0 < 20$ mg.L-1, the apparent first-order rate constant k in the tests can be calculated from the straight line of the plot of ln($C/C_0$) versus illumination time [38]. The experimental results listed in Table1 show that the degradation rate increases with increasing HA concentration, but the apparent kinetic constant k decreases with increasing HA concentration.

### 3.6 HA removal and flux declineconcentration

At the initial stage, HA removal was investigated in photocatalysis batch operation. After three hours of treatment, the solution was transferred to the ultrafiltration cell. Sole ultrafiltration was carried out as well for the purpose of comparison. As shown in Figure 10 (a) 73% of HA was degraded only by photocatalysis, and that UF/photocatalysis experiments improved significantly removal of HA.

The overall process removal efficiency (comprising both HA oxidation and UF membrane filtration was even higher, a removal rate of 95.5 % was achieved after 65 minutes, while 85% were removed by sole filtration. The improvement is due to the reinforcement of ultrafiltration through polyethersulphone membrane by photocatalysis process.

**Table1:** First-order reaction rate constant $k_{app}$ and correlation coefficient R for the photodegradation of HA with different initial concentrations

| $[HA]_0$ (mg.L$^{-1}$) | $K_{app}$ (min$^{-1}$) | R |
|---|---|---|
| 16.9 | 0.00536 ± 4.54601 E-5 | 0.9998 |
| 13.8 | 0.00633 ± 6.53290 E-5 | 0.9997 |
| 7.7 | 0.00835 ± 2.16706 E-4 | 0.9980 |
| 4.1 | 0.00903 ± 1.07462 E-4 | 0.9996 |

Fouling is the main obstacle in filtration process. It reduces membrane productivity and increases the cost of regeneration. The extent of membrane fouling is reflected by flux decline. In this study, the permeate fluxes of HA solution in filtration alone and concurrent process were both monitored to describe the ability of membrane anti-fouling. As expected, no significant flux loss for ultrapure water was achieved Figure 10 (b). In the case of filtration alone, the flux declines from 48.24 initially to 17.68 L/m$^2$ h after ≈ 2.5 h, suggesting cake and HA gel layers formation due to steric hindrance and species adsorption. However, the flux increases to 36.8 L/m$^2$ h by concurrent process. The flux decline observed during the humic acids filtration is due to the combined effects of HA adsorption on membrane surface/pores, HA deposition during filtration, and HA concentration polarization [39]. The coupling which is used allows an almost total retention of catalyst particle.
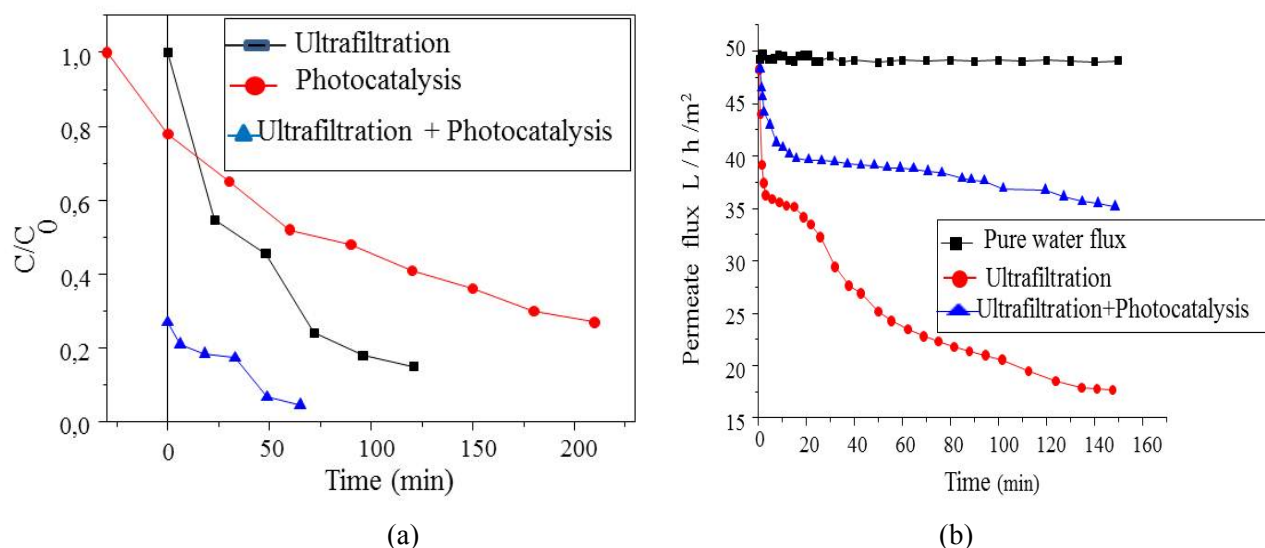


(a)                                    (b)

**Figure 10:** Enhanced performance of integrated photocatalytic degradation and membrane filtration. (Pressure 2 bars, $[HA]_0$ = 10 mg/L and [Mt-Fe] = 0.02 g/L).

## Conclusion

The investigation carried out on photodegradation of humic acids revealed that:
- Photocatalytic process with the use of Mt-Fe as a suspended catalyst was more effective than photolysis process.
- The efficiency of humic acids oxidation during photocatalysis depends on: catalyst dose, exposure time, contaminants concentration and medium pH.
- The new data demonstrates that a hybrid system, combining heterogeneous photocatalysis with suspended Mt-Fe particles and UF membrane filtration, can successfully operate in a 63.5 mm dead-end cell (Model 8200, Amicon Corp.), for the removal of HA. Typical concentrations of HA (10 mg/L) usually encountered in effluents and freshwater sources were degraded. The overall removal efficiency of HA was higher (95.5%) due to the synergistic effects of photocatalysis and membrane filtration processes.

## References

1. A.I. Gomes, J.C. Santos, V.J.P. Vilar, R.A.R. Boaventura, *Appl Catal B*, 88 (2009) 283-291.
2. S.I. Patsios, V.C. Sarasidis, A.J. Karabelas, *Sep Purif Technol*, 104 (2013) 333-341.
3. C.S. Uyguner, S.A. Suphandag, A. Kerc, M. Bekbolet, *Desalination*, 210 (2007) 183-193.
4. S. Valencia, J.M. Marín, G. Restrepo, F.H. Frimmel, *Sci Total Environ*, 442 (2013) 207-214.
5. M. Rajca, M. Bodzek, *Sep Purif Technol*, 120 (2013) 35-42.
6. X. Wang, Z. Wu, Y. Wang, W. Wang, X. Wang, Y. Bu, J. Zhao, *J Hazard Mater*, 262 (2013) 16-24.
7. C.S. Uyguner-Demirel, M. Bekbolet, *Chemosphere*, 84 (2011) 1009-1031.
8. L.A. Galeano, P.F. Bravo, C.D. Luna, M.Á. Vicente, A. Gil, *Appl Catal B*, 111–112 (2012) 527-535.
9. M. EL Alouani, S. Alehyen, M. EL Achouri, M. Taibi *J. Mater. Environ. Sci.*, 9 (2018) 32-46.
10. Y. Morad, M. Hilali, L. Bazzi, A. Chaouay, *Mor. J. Chem.*, 2 (2014) 475-485.
11. G. Chen, G. Luo, X. Yang, Y. Sun, J. Wang, *Mater. Sci. Eng., A Struct Mater*, 380 (2004) 320-325.
12. H.A. El Nazer, S.A. Salman, A.A. Elnazer, *J. Mater. Environ. Sci.*, 8 (2017) 310-317.
13. A. Sarı, *Energy Convers Manag*, 117 (2016) 132-141.
14. A. El Mragui, I. Daou, R. Chfaira, O. Zegaoui *J. Mater. Environ. Sci.*, 8 (2017) 3138-3150.
15. Z. Yang, O. Xiao, B. Chen, L. Zhang, H. Zhang, X. Niu, S. Zhou, *Chem Eng J*, 223 (2013) 31-39.
16. W. Ferjani, L. Khalfallah Boudali *J. Mater. Environ. Sci.*, 7 (2016) 849-858.
17. S. Zuo, M. Ding, J. Tong, L. Feng, C. Qi, *Appl Clay Sci*, 105–106 (2015) 118-123.
18. P. Trikittiwong, N. Sukpirom, W. Chavasiri, *J Mol Catal A Chem*, 378 (2013) 76-81.
19. K.V. Bineesh, M.-I.L. Kim, M.-S. Park, K.-Y. Lee, D.-W. Park, *Catal Today*, 175 (2011) 183-188.
20. P. Yuan, F. Annabi-Bergaya, Q. Tao, M. Fan, Z. Liu, J. Zhu, H. He, T. Chen, *J Colloid Interface Sci*, 324 (2008) 142-149.
21. E.G. Garrido-Ramírez, B.K.G. Theng, M.L. Mora, *Appl Clay Sci*, 47 (2010) 182-192.
22. J. Guo, J. Liu, L.Y. Wang and H. Liu, *Membr. Water Treat., Int. J.*, 6 (2015) 1-13.
23. M. Said, and al., *Membr. Water Treat., Int. J.*, 5 (2014) 207-219.
24. M.W. Naceur, N. Ait Messaoudene, S. Megatli, A. Khelifa, *Desalination*, 168 (2004) 253-258.
25. O. Bouras, J.-C. Bollinger, M. Baudu, *Appl Clay Sci*, 50 (2010) 58-63.
26. A. Ararem, B. Omar, A. Fahd *Chem Eng J*, 172 (2011) 230-236.
27. F. Zermane, B. Cheknane, J.P. Basly, O. Bouras, M. Baudu, *J Colloid Interface Sci*, 395 (2013) 212-216.
28. S. Zhou, C. Zhang, X. Hu, Y. Wang, R. Xu, C. Xia, H. Zhang, Z. Song, *Appl Clay Sci*, 95 (2014) 275-283.
29. G. Xue, H. Liu, Q. Chen, C. Hills, M. Tyrer, F. Innocent, *J Hazard Mater*, 186 (2011) 765-772.
30. W.K. Mekhamer, *J SAUDI CHEM SOC*, 14 (2010) 301-306.
31. B. Makhoukhi, M.A. Didi, H. Moulessehoul, A. Azzouz *MedJChem*, 1 (2011) 44-55.
32. B. Omar, Thesis of Doctor, University of Limoges, (2003).
33. E. Illés, E. Tombácz, *Colloids Surf A Physicochem Eng Asp*, 230 (2003) 99-109.
34. H. Esmaeili, A. Ebrahimi, M. Hajian, H. Pourzamani, *Int J Env Health Eng* 1(2012) 33-33.
35. J. Fu, M. Ji, Z. Wang, L. Jin, D. An, *J Hazard Mater*, 131 (2006) 238-242.
36. F.L. Palmer, B.R. Eggins, H.M. Coleman, *J Photochem Photobiol A Chem*, 148 (2002) 137-143.
37. Z. Khuzwayo, E.M.N. Chirwa, *J Hazard Mater*, 300 (2015) 459-466.
38. X.Z. Li, C.M. Fan, Y.P. Sun, *Chemosphere*, 48 (2002) 453-460.
39. H. Song, J. Shao, J. Wang, X. Zhong, *Desalination*, 344 (2014) 412-421.

(2018) ; http://www.jmaterenvironsci.com